Published in final edited form as:
Exp Cell Res. 2014 May 15; 324(1): 30–39. doi:10.1016/j.yexcr.2014.03.016.

Osteoblastic protein tyrosine phosphatases inhibition and connexin 43 phosphorylation by alendronate

V. Lezcano[a], **T. Bellido**[b,c], **L.I. Plotkin**[b], **R. Boland**[a], and **S. Morelli**[a,*]

[a]Departamento de Biología, Bioquímica y Farmacia, Universidad Nacional del Sur, Bahía Blanca, Argentina

[b]Department of Anatomy and Cell Biology, Indiana University School of Medicine, Indianapolis, IN, USA

[c]Department of Medicine, Division of Endocrinology, Indiana University, Indianapolis, IN, USA

Abstract

Bisphosphonates (BPs), potent inhibitors of bone resorption which inhibit osteoclasts, have also been shown to act on osteocytes and osteoblasts preventing apoptosis via connexin (Cx) 43 hemichannels and activating the extracellular signal regulated kinases ERKs. We previously demonstrated the presence of a saturable, specific and high affinity binding site for alendronate (ALN) in osteoblastic cells which express Cx43. However, cells lacking Cx43 also bound BPs. Herein we show that bound [^{3}H]-alendronate is displaced by phosphatase substrates. Moreover, similar to Na_3VO_4, ALN inhibited the activity of transmembrane and cytoplasmic PTPs, pointing out the catalytic domain of phosphatases as a putative BP target. In addition, anti-phospho-tyrosine immunoblot analysis revealed that ALN stimulates tyrosine phosphorylation of several proteins of whole cell lysates, among which the major targets of the BP could be immunochemically identified as Cx43. Additionally, the transmembrane receptor-like PTPs, RPTPμ and RPTPα, as well as the cytoplasmic PTP1B, are highly expressed in ROS 17/2.8 cells. Furthermore, we evidenced that Cx43 interacts with RPTPμ in ROS 17/2.8 and ALN decreases their association. These results support the hypothesis that BPs bind and inhibit PTPs associated to Cx43 or not, which would lead to the activation of signaling pathways in osteoblasts.

Keywords

Alendronate; Osteoblasts; Cx43 hemichannels; Protein tyrosine phosphatases

Introduction

The bisphosphonates (BPs) are small molecular size (<300 Da) organic pyrophosphate analogues in which two phosphates are connected by a carbon atom (P–C–P) with various side chains. This chemical structure gives them resistance to enzymatic degradation.

*Corresponding author. Fax: + 54 291 4595130. smorelli@criba.edu.ar (S. Morelli).

BPs can be very powerful inhibitors of bone resorption and their potency vary according to their structure. Alendronate (ALN) is a potent amino-BP commonly used in the treatment of osteoporosis.

It is established that BPs inhibit resorption by acting on osteoclasts to reduce their activity or to increase the rate of apoptosis [1]. Several pieces of evidence support the notion that BPs also influence directly the function of cells of the osteoblastic lineage, and that this effect may in turn contribute to the reduction in osteoclast formation and activity. However, the molecular target of ALN, as well as of other BPs, in osteoblasts is still unknown.

It has been previously reported that BPs inhibit osteocyte and osteoblast apoptosis [2]. Moreover, we evidenced that both BPs and the protein-tyrosine phosphatase (PTP) inhibitor Na_3VO_4, increased proliferation of osteoblasts [3]. In addition, we demonstrated in osteoblasts the existence of a saturable, specific and high affinity binding site for the bisphosphonates Olpadronate (OPD) [3] and ALN [4]. In view of these observations, in the present paper we have addressed the possibility that PTPs contain a binding site for BPs.

Protein-tyrosine phosphorylation plays an important role in the signal transduction pathways that control cellular growth, differentiation, and metabolism. Tyrosine phosphorylation levels are controlled by the dynamic equilibrium between the activity of protein-tyrosine kinases (PTK) and PTPs. The latter comprise a diverse family of tyrosine phosphatases which is divided into two main groups: the receptor-like forms, such as CD45 (leukocyte common antigen), RPTPα and RPTPμ; and the cytoplasmic forms, such as PTP1B. Each of the PTPs contains at least one conserved segment of 240 amino acid residues corresponding to the catalytic domain [5]. This study provides information on the expression of these PTP subclasses in ROS 17/2.8 osteoblast-like cells.

Short-term studies in ewes showed that low doses of the phosphatase inhibitor NaF stimulate bone formation by increasing the recruitment and lifespan of osteoblasts [6]. Furthermore, the specific PTP inhibitor orthovanadate, as well as NaF, has been used as anti-osteoporotic drugs in rats and humans, respectively [7,8]. Therefore, we also evaluated herein the effect of the anti-osteoporotic ALN on PTP activity.

The prosurvival effect of BPs in osteoblasts and osteocytes is strictly dependent on the expression of the C-terminal cytoplasmic domain of connexin (Cx) 43, by which the protein interacts with Src kinase, an upstream activator of ERK [9]. However, it is dispensable for ALN cellular binding [4]. The tyrosine phosphatase inhibitor pervanadate inhibits Cx43-based gap junction communication, accompanied by enhanced tyrosine phosphorylation of Cx43 [10,11], but the identity of the PTP(s) that acts (act) on Cx43 remains unknown.

Within the above context, in the present work we propose to elucidate the molecular mechanism involved upstream the signal transduction pathway activated by BPs in osteoblastic cells.

Materials and methods

Reagents

Alendronate was provided by Gador SA. (Buenos Aires, Argentina); *p*-nitrophenylphosphate, phenol red-free αMEM and Na_3VO_4, inhibitor of protein tyrosine phosphatase were from Sigma-Aldrich Co. (St. Louis, MO, USA). Bovine calf serum and fetal bovine serum were from Hyclone (Logan, UT, USA). Alendronate sodium salt [2,3-^{3}H] was from Moravek Biochemicals and Radiochemicals (Brea, CA, USA). AF-488 was provided by Invitro-gen Life Technologies (Grand Island, NY, USA). Rabbit polyclonal antibody recognizing Cx43 and phosphoCx43 (Tyr265) or anti-actin mouse polyclonal antibody were purchased from Sigma-Aldrich Co. (St. Louis, MO, USA). Anti-RPTPα rabbit and anti-PTP1B goat polyclonal antibodies, anti-rabbit and anti-mouse peroxi-dase-conjugated secondary antibodies and protein-G PLUS agarose were from Santa Cruz Biotechnology (Santa Cruz, CA, USA). Anti-RPTPμ, mouse monoclonal antibody was from Cell Signaling (Danvers, MA, USA). Anti-phospho-tyrosine mouse monoclonal antibody was from UBI (NY, USA). Protein size markers, Immobilon P (polyvinylidene difluoride) membranes and ECL chemilumines-cence detection kit were from GE Healthcare (Little Chalfont, Buckinghamshire, England). All other reagents used were of analytical grade.

Cell culture

ROS 17/2.8 osteoblasts (rat osteosarcoma-derived) and HeLa cells were cultured at 37 °C in phenol red-free α-MEM supplemented with 10% FBS, 1% each of penicillin, streptomycin and glutamine, under humidified air (5.5% CO_2) and grown at 70–80% of confluence; 1% minimum essential amino acids were added to the medium for HeLa cells.

Binding assay

Binding of [^{3}H]-alendronate was performed in intact cell mono-layers. ROS 17/2.8 cells were incubated with 30 nM [^{3}H]-alendronate (specific activity 30 Ci/mmol) for 120 min at 30 °C in the absence (total binding) or presence (non-specific binding) of 200 μM unlabeled BPs (Alendronate, ALN; Etidronate, ETI and Olpadronate, OPD), 8 mM *p*-nitro-phenylphosphate or 8 mM α-naftylphosphate, two common protein phosphatase substrates. Results are expressed as a percent of total binding. Each value is the mean ± SD of results from three separate experiments performed in triplicate.

Synthesis of fluorescently labeled alendronate

Alendronate labeled with Alexa Fluor-488 (AF-488) was synthesized in our laboratory following the method described by Thompson et al. [12].

Confocal microscopy

To analyze the uptake of AF-ALN by ROS 17/2.8 cells and its co-localization with RPTPμ, cell cultures grown onto glass coverslips were incubated with AF-ALN for 30 min at the concentration indicated. Subsequently, cells were washed in PBS and fixed for 10 min in 4% (v/v) *p*-formaldehyde and permeabilized with 0.05% Triton X-100. Non-specific sites were blocked with PBS, 5% BSA. Then, cells were incubated with the specific anti-RPTPμ

antibody for 1 h, washed twice with PBS and incubated for additional 1 h in the presence of secondary FITC-conjugated antibody (1:200, room temperature). To determine co-localization of Cx43 and RPTPμ, osteoblastic cells treated with vehicle (control) or 0.1 μM ALN were fixed and incubated with a solution containing anti-Cx43 and anti-RPTPμ, antibodies. Then washed and labeled with specific secondary antibodies. The samples were examined on a Zeiss LSM 5 Pa confocal laser microscope.

Western blot analysis

After the corresponding treatments cells were washed with PBS buffer plus 25 Mm NaF and 1 mM Na_3VO_4, and lysed in buffer A containing 50 mM Tris-HCl (pH 7.4), 150 mM NaCl, 3 mM KCl, 1 mM EDTA, 1% Tween-20, 1% Nonidet P-40, 20 μg/ml aprotinin, 20 μg/ml leupeptin, 1 mM phenylmethylsulfonyl fluoride (PMSF), 25 mM NaF and 1 mM Na_3VO_4. The lysates were incubated on ice for 10 min, vortexed for 45 s and maintained on ice for another 10 min. After centrifugation at 14,000 × *g* and 4 °C during 15 min the supernatant was collected and proteins were quantified using the Bradford method [14]. Lysate proteins dissolved in 6× Laemmli sample buffer containing 4% SDS, 20% glycerol, 10% 2-mercaptoethanol, 0.004% bromphenol blue and 0.125 M Tris HCl [13] were separated (30 μg/lane) by SDS-polyacrylamide gels (10% acrylamide) and electrotransferred to PVDF membranes.

After blocking with 5% non-fat milk in TBST buffer (50 mM Tris pH 7.2–7.4, 200 mM NaCl, 0.1% Tween 20), immunoblottings were performed using a rabbit anti-RPTPα, anti-Cx43 and anti-phospho-Cx43 (Tyr265) antibodies or mouse anti-RPTPμ or anti-PTP1B goat polyclonal antibodies and anti-phospho-tyrosine mouse monoclonal antibody. After washing, blots were exposed to anti-rabbit or anti-mouse or anti-goat antibody conjugated with horseradish peroxidase prepared in TBS-T plus 5% non-fat milk and developed using a chemiluminescence substrate.

Immunoprecipitation

ROS 17/2.8 cells were plated at 80% of confluence in the corresponding growing medium. Lysates (1 mg) obtained as described above (2.6) were precleared with 1 μg of non-immune IgG together with 20 μL protein-G PLUS agarose, for 1 h at room temperature. After centrifugation the immunoprecipitation was carried out in the supernatant with 2 μg of specific antibody (anti-Cx43) together with 20 μL of agarose beads and incubated overnight at 4 °C. The immunoprecipitates were collected by centrifugation and washed three times with lysis buffer (buffer A) without detergent. The pellets were resuspended in 30 μL of 6 × Laemmli sample buffer [13] with DTT and boiled for 5 min. The samples were subject to Western blot analysis using specific antibodies as described above.

Phosphatase assay

PTPases hydrolyze *p*NPP efficiently and their activity was measured as previously described [14]. ROS 17/2.8 cells were lysed in buffer containing 50 mM Tris HCl (pH 7.4), 150 mM NaCl, 3 mM KCl, 1 mM EDTA, 1% Tween-20 and Triton X-100, 20 μg/ml leupeptin and 1 mM phenylmethylsulfonyl fluoride (PMSF). The lysates were incubated on ice for 10 min and vortexed 45 s. After centrifugation at 14,000 × *g* at 4 °C during 15 min the supernatant

was collected and proteins were quantified using the Bradford method [15]. Protein tyrosine phosphatases were immunopreci-pitated by adding 1 μg of appropriate specific antibody to the lysate and incubated ∼7h at 4 °C. Then, 20 μl protein-G PLUS agarose was added and incubated overnight. Each immunopreci-pitated PTP was treated with 0.1 μM ALN, 100 μM Na_3VO_4 or vehicle (control) at 37 °C for 30 min. The negative control was prepared boiling each phosphatase to denature the enzyme. In Fig. 4C, the immunoprecipitated RPTPμ was pre-incubated for 30 min with 0.1 μM ALN, 100 μM Na_3VO_4, ALN+*p*NPP or Na_3VO_4+ *p*NPP. Then, the phosphatase activity assay was performed using *p*NPP as substrate of the enzyme.

Briefly, to evaluate phosphatase activity, the phosphatase assay buffer (100 mM HEPES pH7.5,150 mM NaCl, 1 mM EDTA, 5 mM DTT) was added to all samples followed by 5 μL of *p*NPP (final concentration: 10 mM). The reaction was performed at 30 °C for 30 min and stopped by collecting the supernatant in a tube containing two volumes of 1 N NaOH. The absorbance was read at 405 nm. Results are expressed as a percent over basal activity and presented as the mean±S.D of three experiments with duplicate determinations.

Statistical analysis

Quantitative data are expressed as mean ± standard deviation (SD) from the indicated set of experiments. Statistical differences between means from Figs. 4B and 5III were calculated by the two-tailed Student's t-test [16]. A $p<0.01$ (**) and <0.05 (*) was considered highly statistically significant and statistically significant, respectively. Data from Figs. 1B, 2B, 4A and 4B were first analyzed with one-way ANOVA followed by application of the multiple comparison Bonferroni test to compare means.

Results

Displacement of [^{3}H]-ALN binding by protein phosphatase substrates

Despite the differences in the actions of BPs depending on their chemical structure, we have previously reported the existence of a single population of high affinity and specific binding sites for olpadronate (OPD) [3] as well as for ALN in ROS 17/2.8 osteoblastic cells, primary cultures of rat osteoblasts and MLO-Y4 osteocytes by competitive binding assays [4]. Because BPs resemble the naturally occurring pyrophosphate (PPi), protein phosphatases might be good molecular candidates for BP binding. To study this topic in depth, we performed competitive binding assays with tritiated alendronate ([^{3}H]-ALN) in the presence (nonspecific) or absence of different unlabeled BPs and phosphatase substrates. We found that OPD inhibited the [^{3}H]-ALN binding with an IC50 of 0.67 μM ± 0, 21 (Fig. 1A) similar to ALN, while ETI showed less potent inhibition (IC50=1.2 μM ± 0, 26). Likewise, 8 mM of the phosphatase substrates *p*-nitrophenylphosphate (*p*-NPP) or α-naphtylphosphate (α-NP) significantly displaced [^{3}H]-ALN binding in ROS 17/2.8 cells, with 68 ± 14% and 95±4% of displacement, respectively (Fig. 1B).

Osteoblastic protein tyrosine phosphatases basal expression and activity inhibition by ALN

Since there is little evidence on the expression of tyrosine phosphatases in bone cells, we evaluated by Western blot analysis the presence of the PTPs of interest in osteoblastic cells. Among all the PTPs existing, this study was focused on PTPs with a different subcellular localization, related to bone metabolism and bisphosphonates [17,18]. We found that ROS 17/2.8 cells express transmembrane RPTPα and RPTPμ as well as cytoplasmic PTP1B (Fig. 2A).

Taking into account the molecular structure of BPs and that ALN bound to osteoblastic cells was displaced by phosphatase sub-strates, we further investigated the mechanism of action of ALN in osteoblasts by evaluating its effect on the phosphatase activity of the PTPs expressed in ROS 17/2.8 cells.

We performed a cell-free assay treating the PTP immune com-plexes with ALN or orthovanadate as a control of phosphatase activity inhibition. The results indicate that both ALN and the well-known PTP inhibitor Na_3VO_4 were capable of significantly inhibit-ing the activity of the above three PTPs with a different cellular localization possessing homologous catalytic domains. The highest effects of ALN were observed on the transmembrane RPTPα and RPTPμ, with ∼40% and ∼50% inhibition of their basal activity, respectively. The cytoplasmic PTP1B was inhibited to a lesser extent (20%) by ALN (Fig. 2B).

AF-ALN is internalized by osteoblast-like cells and co-localizes with RPTPμ

Because the catalytic domain of all the PTPs has an intracellular localization [19], we studied by confocal microscopy if ALN is internalized into non-resorbing bone cells. Moreover, we investigated whether ALN co-localizes with one of the PTPs studied, RPTPμ. To carry out these experiments we synthesized ALN labeled with the fluorescent probe Alexa Fluor 488 (AF-ALN) following the method described by Thompson et al. [12]. ROS 17/2.8 cells were incubated in the presence of 0.1 μM AF-ALN for 30 min and then incubated with the specific antibody that recognizes RPTPμ. The phase contrast image showed that this protocol did not affect the characteristic morphology of osteo-blastic cells (Fig. 3A). AF-ALN was observed throughout the cytosol (Fig. 3B), indicating that ALN is rapidly incorporated by the osteoblasts. RPTPμ was detected overall the cytoplasm (Fig. 3C) and the merge of images demonstrated co-localization of both, AF-ALN and RPTPμ (Fig. 3D).

Tyrosine phosphorylation levels in response to ALN

Taking into account the inhibition of PTPs activity observed in response to ALN, we then investigated the tyrosine phosphorylation levels in whole cell lysates obtained from ROS 17/2.8 cells. The cells were treated for 30 min in the absence (control) or presence of 0.1 μM ALN, 100 μM Na_3VO_4 or the co-treatment of each of them with 10 mM *p*NPP, a phosphatase substrate. Whole cell lysates were then analyzed by Western blotting using an antibody detecting phospho-tyrosine-containing proteins. The blot and its corresponding quantification shown in Fig. 4A demonstrated that ALN significantly increased the tyrosine

phos-phorylation of various cellular proteins. Significant changes in phosphotyrosine-containing proteins of relative molecular masses of 35–50 kDa were observed in response to ALN and Na_3VO_4. When cells were treated with BP or Na_3VO_4, both co-incubated with *p*NPP, we observed an increase in tyrosine phosphorylation levels, and, in addition, the co-treatment of ALN with *p*NPP reversed the inhibitory effect of the BP on the RPTPμ activity. The latter is represented by Fig. 4C, which evidences that ALN and the tyrosine phosphatase inhibitor Na_3VO_4, significantly decrease RPTPμ activity compared to basal (38.5% and 57.3%; respectively); and, when each compound was co-incubated with *p*NPP, the levels of phosphatase activity significantly increased over basal condition (∼140%).

There is previous evidence correlating the phosphorylation levels of connexin 43 (Cx43) with the opening and closure of this hemichannel [20]; and it was demonstrated by other authors that ALN modify this gating state leading to the activation of signaling pathways related to the anti-apoptotic effects of BPs in osteocytes [9]. To evaluate in particular the effect of ALN on Cx43 phosphorylation levels, whole cell lysates were immunoprecipitated with anti-total Cx43 and analyzed by immunoblot with anti-phosphotyrosine and anti-total Cx43 as loading control (Fig. 4B). The representative blots and their corresponding quantification indicate, as expected, that ALN increases the phosphorylation levels of Cx43 in tyrosine residues.

ALN decreases RPTPμ-Cx43 co-localization in osteoblasts

It was previously reported that the catalytic domain of RPTPμ from mink lung cells interacts with Cx43 in basal conditions, suggesting that Cx43 is a physiological substrate for RPTPμ [20]. To further investigate the association of RPTPμ and Cx43 in osteoblastic cells we studied the co-localization of these two proteins by confocal microscopy. ROS 17/2.8 cells were treated with vehicle (control) or 0.1 μM ALN, then fixed and incubated with anti-Cx43 (Ser265) antibody together with anti-RPTPμ antibody. To distinguish each protein in the same field, specific secondary antibodies conjugated with different fluorophores were employed. Negative controls were included for which fixed cells were incubated with secondary antibodies in the absence of primary antibody *(data not shown)*. Confocal microscopy images show that phosphorylated Cx43 localizes throughout the cell (Fig. 5I; A and D). Since this protein has its main function as hemichannel-forming protein, we expected plasmatic membrane localization. To exclude unspecific interactions of anti-Cx43 we induced the expression of Cx43-GFP fusion protein in Cx43-deficient HeLa cells (Fig. 5II). These cells showed a cellular distribution of Cx43 comparable to that observed by immunocy-tochemistry of osteoblastic cells.

RPTPμ was also distributed throughout the cell (Fig. 5I; B and E). The merge of images indicated that phospho-Cx43 co-localizes with RPTPμ (Fig. 5I; C) and this co-localization decreased (20% of control) after 30 min of ALN treatment (Fig. 5I; F).

Discussion

Performing whole cell binding assays with [^{3}H]-ALN, we previously demonstrated the presence of a saturable, specific and high affinity binding site in ROS 17/2.8 osteoblastic cells and rat calvaria-derived osteoblasts [4]. Other BPs were as effective as ALN in

displacing [^{3}H]-ALN and exhibited comparable affinity binding site, suggesting a similar behavior as ligands in osteoblasts, despite their differences in chemical structure. Of relevance, in this study we found that [^{3}H]-ALN bound to ROS 17/2.8 cells was displaced by phosphatase substrates, indicating that the catalytic domain of phosphatases might be the binding site of ALN.

The requirement of Cx43 for anti-apoptosis by BPs has raised the possibility that interaction of bisphosphonates with Cx43 present in the cell membrane results in hemichannel opening, thereby initiating intracellular survival signaling. However, we previously found that, although Cx43 is necessary for BP-induced survival of osteoblastic cells, this protein is dispensable for BP cell binding [4]. Thus, BPs can bind to cells lacking Cx43 or cells in which connexin channels have been disrupted, suggesting that the drugs bind to another moiety that, in turn, interacts with Cx43. Because herein we demonstrated that ALN binding to osteoblastic cells is displaced by protein phosphatase substrates, the unknown molecule which links BPs with Cx43 could be a phosphatase.

There is growing evidence that tyrosine phosphorylation is involved in the regulation of a number of important cellular processes such as growth, movement, adhesion and oncogenic transformation [21–23]. The steady-state level of cellular tyrosine phosphorylation is obviously dependent on the balance of PTPase and tyrosine kinase activities. There has been recently considerable progress in the characterization of cellular PTPases. These molecules are now known to belong to a multimembered family composed of non-receptor (cytosolic) and receptor-like (cell-membrane-spanning) forms [5,24]. PTPases share regions of homology including a well-conserved active domain. However, there is little information about their regulation. In this study we have obtained evidence that ROS 17/2.8 osteoblastic cells express at least three PTPs, including two membrane-associated and one cytosolic. We demonstrated by means of phosphatase assays that both ALN and the PTP inhibitor Na_3VO_4 were capable to inhibit the activity of these PTPs. This leads to the conclusion that ALN not only binds to PTPs but also inhibits their activity. The fact that RPTPμ, RPTPα and PTP1B were all inhibited by ALN raises the possibility that the BP has not a specific PTP target. Accordingly, it has been shown that BPs also inhibit the activity of PTPs from osteoclasts *in vitro*. Moreover, this effect appears to be restricted to PTPs, since BPs do not inhibit other enzymes involved in phosphate metabolism [17]. Consistent with the above information, in this work we demonstrated that ALN, as well as the commonly used PTP inhibitor Na_3VO_4, increases the phosphorylation levels in tyrosine residues from whole cell lysates of osteoblastic cells; specifically, the phosphorylation of a group of proteins with a molecular weight pattern suggestive of Cx43. In addition, ALN increases Cx43 phosphorylation levels in tyrosine residues, probably due to the absence of PTPs activity. Previous work of the authors has demonstrated that the pro-survival effect of ALN in osteoblasts is strictly dependent on the C-terminal domain of Cx43, which contains the phosphorylation sites of this protein [25]. Further studies might be performed to directly correlate the latter with the increase in tyrosine phosphorylation. Altogether, these results support the idea that ALN acts as a PTP inhibitor by binding to the catalytic domain of the phosphatases. Previous studies [9] and this model provide for the transient nature of the hemichannel opening by bisphosphonates. We propose that ALN induces the opening of Cx43, enters to the cell

through an unknown molecule [4] and then interacts with molecules which lead to the hemichannel closure by phosphorylation of the C-terminal portion, due to kinases activation (Src and ERKs) [9] and/ or PTPs inhibition.

It has been established that the catalytic domain of all the PTPs has an intracellular localization [19]. In agreement with the above observations, we confirmed by confocal microscopy our hypothesis that ALN is internalized into non-resorbing bone cells. Moreover, we found that intracellular AF-ALN co-localizes with one of the PTPs studied which showed high levels of expression in ROS 17/2.8 cells, namely RPTPμ. Interestingly, AF-ALN cellular uptake as well as PTP inhibition and co-localization of ALN with RPTPμ occurred at the same time point, within 30 min of treatment.

Many of the connexins not only contain protein kinase “consensus phosphorylation sequences”, but have also been demonstrated to be phosphorylated in the C-terminal region that is located in the cytoplasm. In this regard, Lampe et al. [26] demonstrated that connexins are targeted by numerous protein kinases, some of which have been identified: protein kinase C, mitogen-activated protein kinase, and the v-Src tyrosine protein kinase. Consistent with these results, Plotkin et al. [9] previously reported that the Cx43 C-terminal portion of the molecule serves as the docking site for Src kinase (s) or other adaptor molecules. The subsequent Src activation links Cx43 with the ERK pathway, which would lead to closure of Cx43 hemichannels and preservation of cellular homeostasis.

Although protein kinases have an established role in the phosphorylation status of Cx43, less is known about the involvement of protein phosphatases. The identity of the PTP(s) that act(s) on Cx43 remains unknown. Attractive candidates, however, are the receptor-like PTPs (RPTPs) with an ectodomain that mediates homotypic cell-cell interaction [27,28], such as RPTPμ [29,30]. Giepmans et al. [31] showed that RPTPmu interacts with Cx43 in lung cells transfected with the hemichannel, keeping Cx43 in a tyrosine-dephosphorylated state.

In line with the above information, we corroborated by co-immunoprecipitation assays endogenous association of Cx43 with the transmembrane RPTPμ in osteoblastic cells (data not shown). This suggests that Cx43 might be a physiological substrate for RPTPμ in ROS 17/2.8 cells; and would explain the increase of Cx43 tyrosine phosphorylation levels observed in osteoblastic cells subjected to ALN treatment. The presence of high concentrations of the phosphatase substrate pNPP demonstrated a complete reversion of the inhibitory effect that ALN showed on PTP activity, indicating that the BP would behave as a typical competitive inhibitor which binds to the active site of phosphatases.

To obtain additional evidence, we evaluated co-localization of these two proteins in ROS 17/2.8 cells by confocal microscopy. Basal co-localization of Cx43 with RPTPμ was observed, confirming the preceding result. Furthermore, ALN treatment induced a decrease in this co-localization suggesting that the BP might be occupying the catalytic domain of PTPs avoiding the association with Cx43 phosphorylation sites. Further investigations should be performed to confirm this interpretation.

Nowadays, protein tyrosine kinases and PTPs are regarded as corporate enzymes that coordinate the regulation of signaling responses, sometimes even by acting in concert [32].

The inhibition of PTPs by BPs could result in an imbalance of the general phosphorylation state of proteins or a sustained phosphorylation by protein kinases that in turn lead to activation of mitogenic pathways in osteoblastic cells. In keeping with this proposal we have previously reported that BPs stimulate osteoblast proliferation via PTPs [3,4].

In conclusion, our findings suggest that ALN is internalized by osteoblastic cells through a mechanism not elucidated yet, binds to the catalytic domain and inhibits the activity of PTPs, such as RPTPμ, that in turn associates with Cx43, increasing its tyrosine phosphorylation levels and triggering the activation of intracellular signaling pathways in bone cells (Fig. 6). Such events would then lead to prevention of apoptosis and stimulation of proliferation as previously shown [2,4]. These studies contribute to further understand the upstream molecular actions of ALN in osteoblasts and raise the possibility of PTPs as potential new class of therapeutic targets.

Preservation of the bone-forming function of mature osteoblasts and maintenance of the osteocytic network, in combination with the inhibition of osteoclasts actions, open new therapeutic possibilities for bisphosphonates in the correct treatment of osteopenic conditions in which increased bone resorption needs to be avoided.

Acknowledgments

The authors thank A. Colicheo for technical assistance. This research was supported by grants from the National Institutes of Health (FIRCA R03 TW006919) to Drs. Teresita Bellido and Ricardo Boland, and from the Florencio Fiorini Foundation and the Universidad Nacional del Sur (PGI 24/B161) to Dr Susana Morelli.

Abbreviations

BPs	bisphosphonates
ALN	alendronate
OPD	olpadronate
ETI	etidronate
PPi	inorganic pyrophosphate
PTP	protein tyrosine phosphatase
RPTP	receptor-like PTP
***p*NPP**	*p*-nitrophenylphosphate
AF-ALN	fluorescently labeled (Alexa Fluor-488) analog of alendronate
[^{3}H]-ALN	tritiated alendronate
Cx43	connexin 43; phosphatase inhibitor
NaF	sodium fluoride; phosphatase inhibitor
Na_3VO_4	orthovanadate

REFERENCES

1. Rogers MJ. From molds and macrophages to mevalonate: a decade of progress in understanding the molecular mode of action of bisphosphonates. Calcif. Tissue Int. 2004; 75:451–461. [PubMed: 15332174]
2. Plotkin LI, Weinstein RS, Parfitt AM, Roberson PK, Manolagas SC, Bellido T. Prevention of osteocyte and osteoblast apoptosis by bisphosphonates and calcitonin. J. Clin. Invest. 1999; 104:1363–1374. [PubMed: 10562298]
3. Morelli S, Scodelaro Bilbao P, Katz S, Lezcano V, Roldán E, Boland R, Santillán GE. Protein phosphatases: possible bosphosphonate binding sites mediating stimulation of osteoblast proliferation. Arch. Biochem. Biophys. 2011; 507:248–253. [PubMed: 21167123]
4. Lezcano V, Bellido T, Plotkin LI, Boland R, Morelli S. Role of connexin 43 in the mechanism of action of alendronate: dissociation of anti-apoptotic and proliferative signaling pathways. Arch. Biochem. Biophys. 2012; 518:95–102. [PubMed: 22230328]
5. Neel BG, Tonks NK. Protein tyrosine phosphatases in signal transduction. Curr. Opin. Cell. Biol. 1997; 9:193–204. [PubMed: 9069265]
6. Chavassieux P, Pastoureau P, Boivin G, Chapuy MC, Delmas PD, Meunier PJ. Dose effects on ewe bone remodeling of short-term sodium fluoride administration - a histomorphometric and biochemical study. Bone. 1991; 12:421–427. [PubMed: 1797057]
7. Hulley PA, Conradie MM, Langeveldt CR, Hough FS. Glucocorticoid-induced osteoporosis in the rat is prevented by the tyrosine phosphatase inhibitor, sodium orthovanadate. Bone. 2002; 31:220–229. [PubMed: 12110438]
8. Devogelaer JP, De Deuxchaisnes CN. Fluoride therapy of type I osteoporosis. Clin. Rheumatol. 1995; 14:26–31. [PubMed: 8846658]
9. Plotkin LI, Manolagas SC, Bellido T. Transduction of cell survival signals by connexin-43 hemichannels. J. Biol. Chem. 2002; 277:8648–8657. [PubMed: 11741942]
10. Mikalsen SO, Kaalhus O. A characterization of pervanadate, an inducer of cellular tyrosine phosphorylation and inhibitor of gap junctional intercellular communication. Biochim. Biophys. Acta. 1996; 1290:308–318. [PubMed: 8765135]
11. Postma FR, Hengeveld T, Alblas J, Giepmans BN, Zondag GC, Jalink K, Moolenaar WH. Acute loss of cell-cell communication caused by G protein-coupled receptors: a critical role for c-Src. J. Cell. Biol. 1998; 140:1199–1209. [PubMed: 9490732]
12. Thompson K, Rogers MJ, Coxon FP, Crockett JC. Cytosolic entry of bisphosphonate drugs requires acidification of vesicles following fluid-phase endocytosis. Mol. Pharmacol. 2006; 69:1624–1632. [PubMed: 16501031]
13. Laemmli UK. Cleavage of structural proteins during the assembly of the head of bacteriophageT4. Nature. 1970; 227:680–685. [PubMed: 5432063]
14. Tonks NK, Diltz CD, Fischer EH. Characterization of the major protein-tyrosine-phosphatases of human placenta. J. Biol. Chem. 1988; 263:6731–6737. [PubMed: 2834387]
15. Bradford MM. A rapid and sensitive method for quantification of microgram quantities of proteins utilizing the principle of protein binding. Anal. Biochem. 1976; 72:248–254. [PubMed: 942051]
16. Snedecor, GW.; Cochran, WG. Statistical Methods. 6th ed. Ames, Iowa: Iowa State University Press; 1967.
17. Schmidt A, Rutjedge J, N Endo, Opas E, Tanaka H, Weso-lowski G, Leu C, Huang Z, Ramachandaran C, Rodan S, Rodan G. Protein tyrosine phosphatase activity regulates osteoclast formation and function: inhibition by alendronate. Proc. Natl. Acad. Sci. 1996; 93:3068–3073. [PubMed: 8610169]
18. Rodan GA, Fleisch HA. Bisphosphonates: mechanisms of action. J. Clin. Invest. 1996; 97:2692–2696. [PubMed: 8675678]
19. Tabernero L, Aricescu AR, Jones YE, Szedlacsek SE. Protein tyrosine phosphatases: structure-function relationships. FEBS J. 2008; 275:867–882. [PubMed: 18298793]
20. Giepmans BN, Feiken E, Gebbink MF, Moolenaar WH. Association of connexin43 with a receptor protein tyrosine phosphatase. Cell Commun. Adhes. 2003; 10:201–205. [PubMed: 14681016]

21. Hanks SK, Calalb MB, Harper MC, Patel SK. Focal adhesion protein-tyrosine kinase phosphorylated in response to cell attachment to fibronectin. Proc. Natl. Acad. Sci. 1992; 89:8487–8491. [PubMed: 1528852]
22. Makgoba MW, Bernard A, Sanders ME. Cell adhesion/signalling: biology and clinical applications. Eur. J. Invest. 1992; 22:443–453.
23. Guan JL, Shalloway D. Regulation of focal adhesion-associated protein tyrosine kinase by both cellular adhesion and oncogenic transformation. Nature. 1992; 358:690–692. [PubMed: 1379699]
24. Fischer EH, Charbonneau H, Tonks NK. Protein tyrosine phosphatases: a diverse family of intracellular and transmembrane enzymes. Science. 1991; 253:401–406. [PubMed: 1650499]
25. Bellido T, Plotkin LI. Novel actions of bisphosphonates in bone: preservation of osteoblast and osteocyte viability. Bone. 2011; 49(1):50–55. [PubMed: 20727997]
26. Lampe PD, Lau AF. Regulation of Gap Junctions by Phosphorylation of Connexins. Arch. Biochem. Biophys. 2000; 384:205–215. [PubMed: 11368307]
27. Brady-Kalnay SM, Tonks NK. Protein tyrosine phosphatases as adhesion receptors. Curr. Opin. Cell Biol. 1995; 7:650–657. [PubMed: 8573339]
28. Zondag GC, Moolenaar WH. Receptor protein tyrosine phosphatases: involvement in cell-cell interaction and signaling. Biochimie. 1997; 79:477–483. [PubMed: 9451448]
29. Brady-Kalnay SM, Flint AJ, Tonks NK. Homophilic binding of PTP mu, a receptor-type protein tyrosine phosphatase, can mediate cell-cell aggregation. J. Cell. Biol. 1993; 122:961–972. [PubMed: 8394372]
30. Gebbink MF, Zondag GC, Koningstein GM, Feiken E, Wubbolts RW, Moolenaar WH. Cell surface expression of receptor protein tyrosine phosphatase RPTPmu is regulated by cell-cell contact. J. Cell. Biol. 1995; 131:251–260. [PubMed: 7559782]
31. Giepmans BN. Gap junctions and connexin-interacting proteins. Cardiovasc. Res. 2004; 62:233–245. [PubMed: 15094344]
32. Hendriks WJ, Elson A, Harroch S, Stoker AW. Protein tyrosine phosphatases: functional inferences from mouse models and human diseases. FEBS J. 2008; 275:816–830. [PubMed: 18298790]

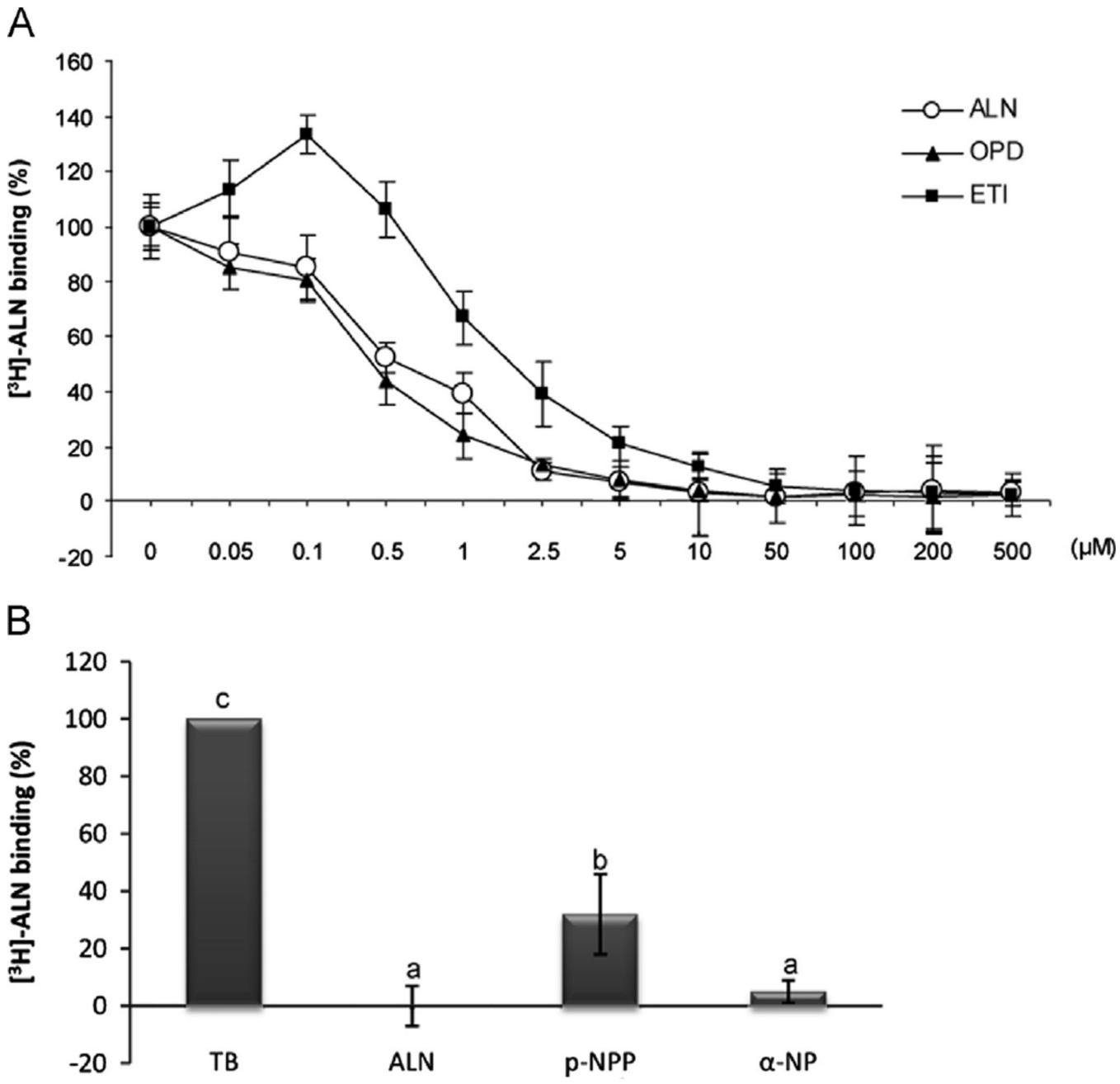

Fig. 1.

Displacement of osteoblast [^{3}H]-ALN binding by other BPs and protein phosphatase substrates. (A) ROS 18/2.8 osteoblastic cells were incubated with 30 nM [3 H]-ALN in the presence of different concentrations (0–500 μM) of unlabeled BPs: ETI (▪), OPD (▲) and ALN (o). Each value is the mean±SD of results from three separate experiments performed in triplicate. B) ROS 17/2.8 cells were incubated with 30 nM [^{3}H]-ALN in the absence (total binding, TB) or presence of 200 μM unlabeled ALN or 8 mM of the phosphatase substrates p-nitro-phenylphosphate (p-NPP) or α-naftylphosphate (α-NP). Results expressed as a percent of total binding are the average±SD. Data were analyzed by one-way analysis of

variance, and the Bonferroni test was used for mean comparison. *Same letters* indicate $p>0.05$, whereas *different letters* indicate $p<0.05$.

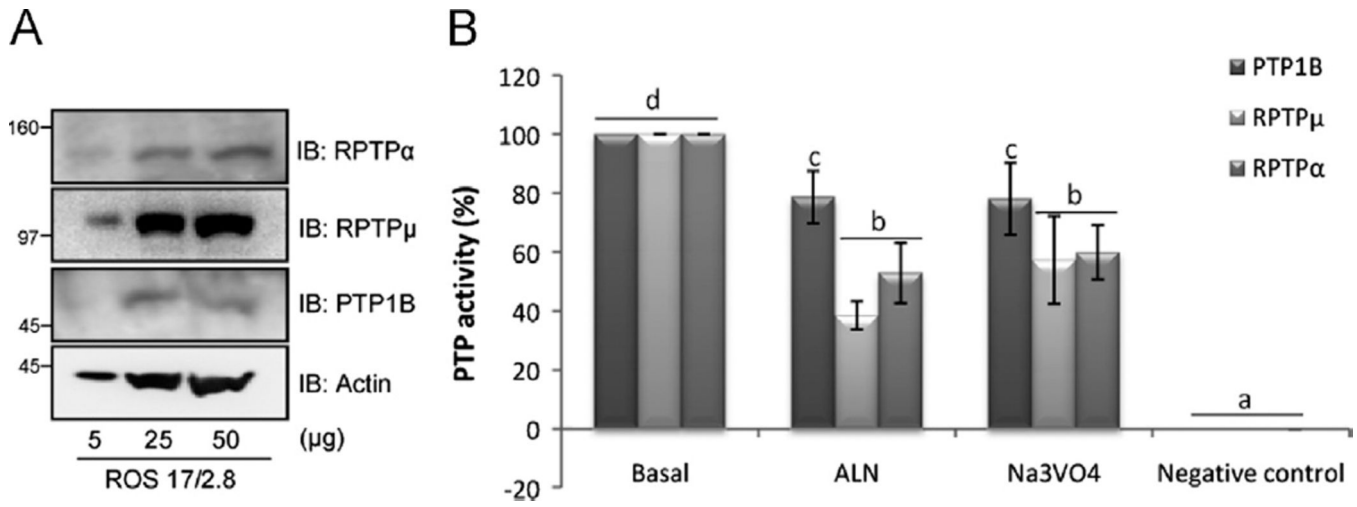

Fig. 2.

Osteoblastic protein tyrosine phosphatases basal expression and activity inhibition by ALN. (A) Detection of basal protein expression of RPTPμ, RPTPα and PTP1B in lysates obtained from ROS 17/2.8 cell line, using Western blot analysis. Different amounts of proteins were loaded and specific antibodies were employed. (B) Cell-free studies were performed. RPTPα, RPTPμ and PTP1B were first immunoprecipitated by adding the appropriate specific antibody to 700 μg of total protein lysate obtained from ROS 17/2.8 cells and incubated overnight with protein-G PLUS agarose. Treatments were then performed directly on the PTP isolated and the negative control was prepared boiling each phosphatase to denaturalize the enzyme. The phosphatase assay was carried out at 37 °C for 30 min by the addition of the substrate *p*NPP (10 mM) and the release of the colored product was measured at 405 nm. Results are expressed as percentage of basal activity and the data are the average±SD of values from three separate experiments. Data were analyzed by one-way analysis of variance, and the Bonferroni test was used for mean comparison. *Same letters* indicate $p>0.05$, whereas *different letters* indicate $p<0.05$.

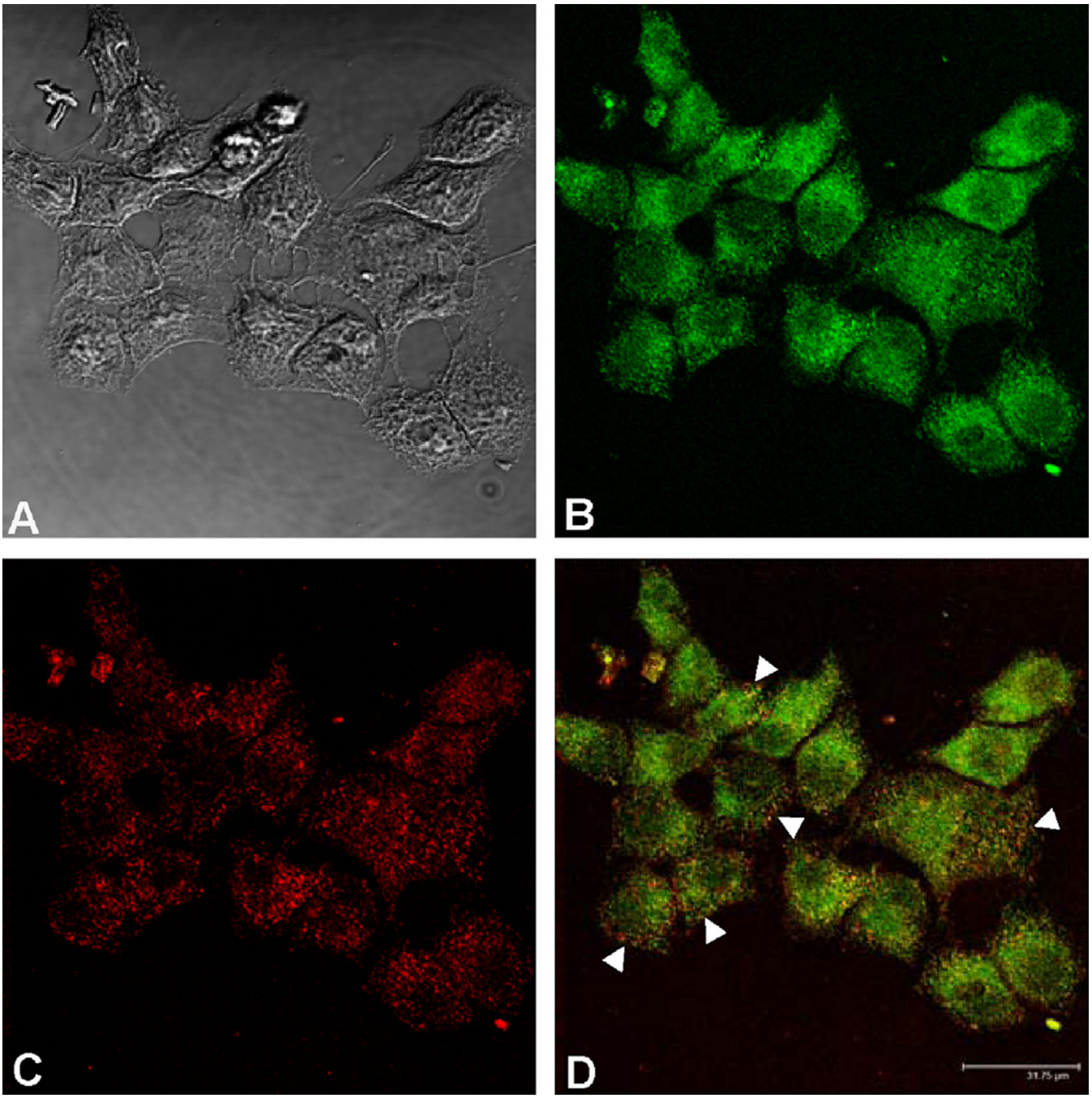

Fig. 3.

AF-ALN is internalized by osteoblast-like cells and co-localizes with RPTPμ. To visualize the uptake of ALN by osteoblastic cells and its co-localization with a phosphatase, ROS 17/2.8 cells were incubated for 30 min with 0.1 μM Alexa Fluor 488-ALN (green), then fixed and incubated overnight with a specific antibody that recognizes RPTPμ, followed by an appropriate dilution of secondary antibody labeled with Alexa Fluor-647 (red). The samples were analyzed by confocal microscopy (scale bar, 31.75 μm). Phase contrast image (A); AF-ALN (B); RPTPμ (C); merge image showing co-localization (arrows) of pixels in

yellow (D). (Images A and B are reprinted with kind permission of Elsevier, Archives of Biochemistry and Biophysics, 518 (2012) 95–102, Lezcano, Bellido, Plotkin, Boland and Morelli).

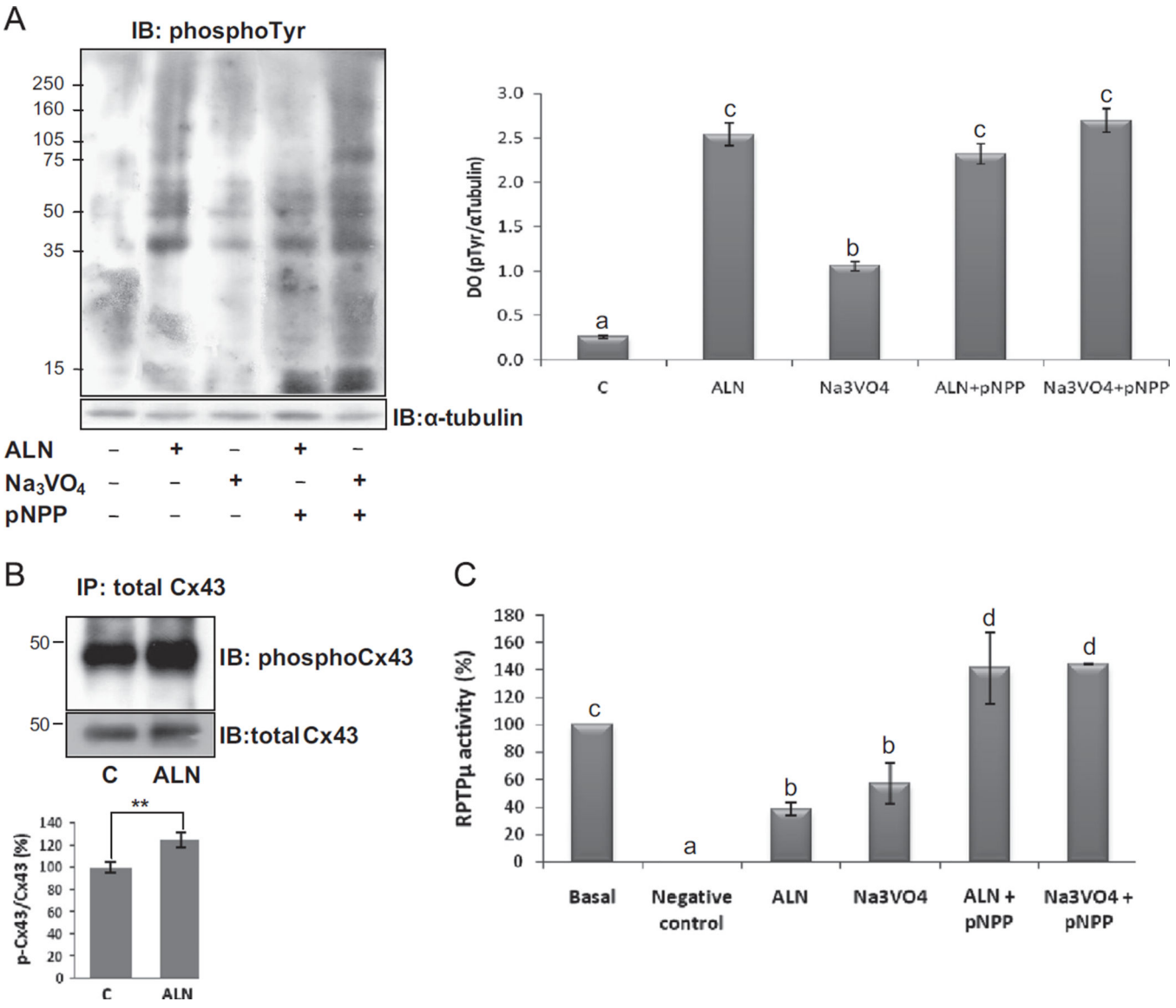

Fig. 4.

Tyrosine phosphorylation levels and RPTPμ activity in response to ALN. (A) ROS 17/2.8 cells were treated for 30 min with vehicle, 0.1 μM ALN, 100 μM Na_3VO_4, 0.1 μM ALN+10 mM phosphatase substrate (*p*NPP) or 100 μM Na_3VO_4+10 mM *p*NPP. Then, cell lysates were performed and tyrosine phosphorylation was evaluated by Western blot analysis using anti-phospho tyrosine antibody. α-tubulin antibody was employed for loading control. The blots are representative of three independent experiments. Densitometric quantification of phospho-tyrosine proteins ranging from 35–75 kDa and normalized with the loading control is showed in the bars graphic. (B) Cells were treated for 30 min in the absence (control; C) or presence of 0.1 μM ALN. Then, cells were lysed and immunoprecipitated with a monoclonal anti-Cx43 antibody. Afterwards, samples were subjected to Western blot analysis and probed for phospho-Cx43 (Tyr265) with a specific antibody. Total Cx43 antibody was employed as loading control. The blots are representative of three independent experiments and densitometric quantification of phospho-Cx43 normalized with the loading

control is showed in the bars graphic. **$p<0.01$ vs. control. (C) RPTPμ was immunoprecipitated from ROS 17/2.8 cell lysates, and then treated for 30 min with vehicle (basal), 0.1 μM ALN, 100 μM Na_3VO_4, 0.1 μM ALN+10 mM *p*NPP or 100 μM Na3VO4+10 mM *p*NPP. The PTP activity was determined as described in Methods. Results are expressed as percentage of basal activity and the data are the average ± SD of values from three separate experiments. Data from graphics B and C were analyzed by one-way analysis of variance, and the Bonferroni test was used for mean comparison. *Same letters* indicate $p > 0.05$, whereas *different letters* indicate $p<0.05$.

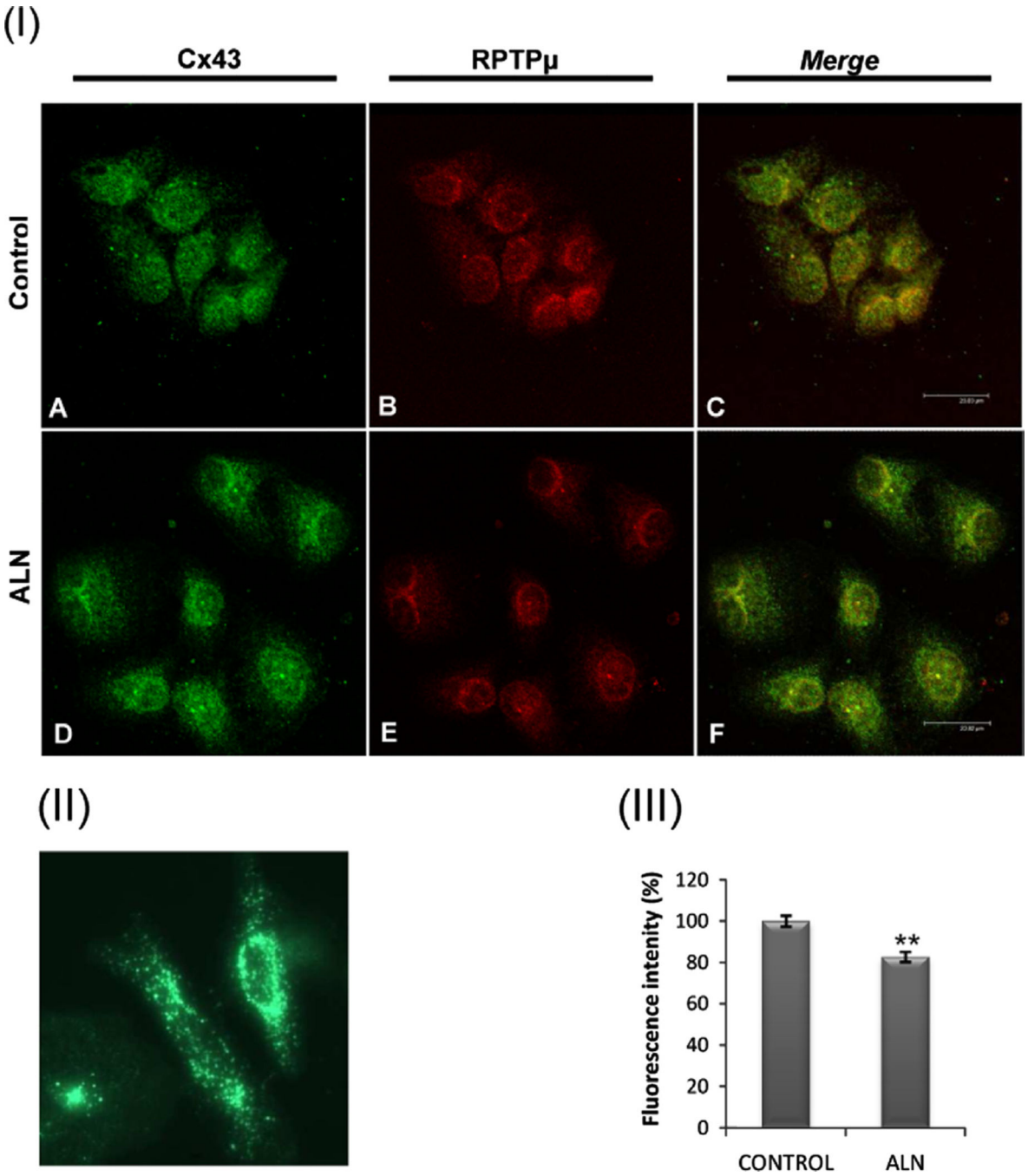

Fig. 5.

ALN decreases RPTPμ-Cx43 co-localization in osteoblasts. (I) ROS 17/2.8 cells were incubated with vehicle (A–C) or 0.1 μM alendronate (D–F) for 30 min. Then, cells were fixed, permeabilized, double-label immunostained using rabbit anti-Cx43 (Tyr265) (A and D - *green)* and mouse anti- RPTPμ (B and E - *red)* and detected using specific secondary antibodies conjugated with different fluorophores. Samples were analyzed by confocal microscopy (scale bar, 23.83 μm). Merged image demonstrates co-localization as yellow pixels (C and F - *merge*). (II) HeLa cells which lack endogenous Cx43 were transfected with

a plasmid containing the Cx43-GFP fusion protein. (III) To quantify fluorescence of images C and F, the summed pixel intensity was calculated by delimiting each region per cell using ImageJ software. Relative values of fluorescence were obtained and expressed as a percentage of fluorescence intensity. The results are shown as mean+S.D. (n=20). **p<0.01, with respect to the control.

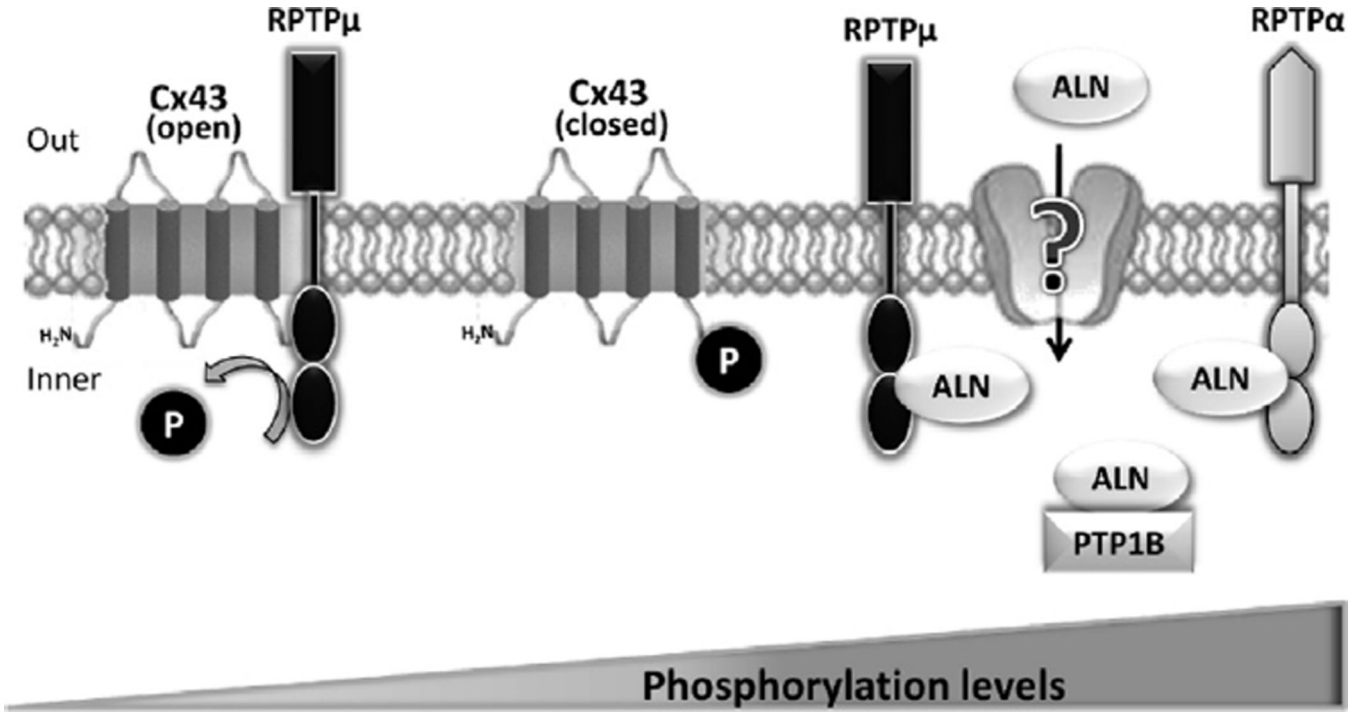

Fig. 6.

Proposed model for bisphosphonate action in osteoblastic cells. Based on the present and previous findings, we propose that bisphosphonates are internalized by osteoblastic cells through a mechanism not yet elucidated, bind and inhibit protein tyrosine phosphatases (e.g. RPTPμ) that in turn interact with connexin 43, increasing tyrosine phosphorylation levels and triggering the activation of intracellular signaling which leads to a biological response such as proliferation.